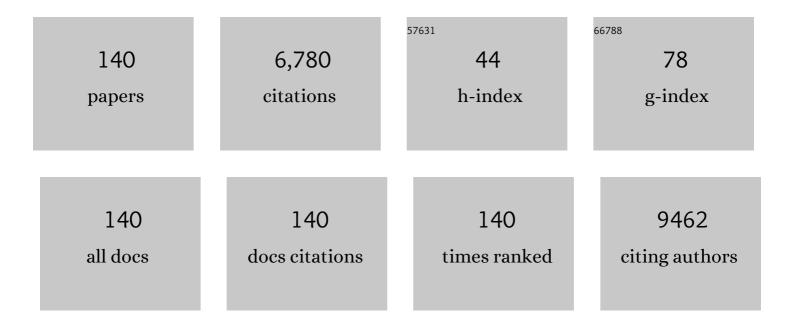
Yit-Tsong Chen

List of Publications by Year in descending order

Source: https://exaly.com/author-pdf/5365321/publications.pdf Version: 2024-02-01



#	Article	IF	CITATIONS
1	<i>In Situ</i> Spectroelectrochemical Detection of Oxygen Evolution Reaction Intermediates with a Carboxylated Graphene–MnO ₂ Electrocatalyst. ACS Applied Materials & Interfaces, 2022, 14, 5177-5182.	4.0	14
2	Nearâ€Infrared Electroluminescent Lightâ€Emitting Transistors Based on CVDâ€Synthesized Ambipolar ReSe ₂ Nanosheets. Advanced Optical Materials, 2022, 10, .	3.6	3
3	Zn2+-Depletion Enhances Lysosome Fission in Cultured Rat Embryonic Cortical Neurons Revealed by a Modified Epifluorescence Microscopic Technique. Microscopy and Microanalysis, 2021, 27, 420-424.	0.2	0
4	A Bi-Anti-Ambipolar Field Effect Transistor. ACS Nano, 2021, 15, 8686-8693.	7.3	30
5	Significant Elevation in Potassium Concentration Surrounding Stimulated Excitable Cells Revealed by an Aptamer-Modified Nanowire Transistor. ACS Applied Bio Materials, 2021, 4, 6865-6873.	2.3	2
6	Detecting glycated hemoglobin in human blood samples using a transistor-based nanoelectronic aptasensor. Nano Today, 2021, 41, 101294.	6.2	12
7	N- and S-codoped graphene hollow nanoballs as an efficient Pt-free electrocatalyst for dye-sensitized solar cells. Journal of Power Sources, 2020, 449, 227470.	4.0	22
8	Stoichiometry-Controlled Mo <i>_x</i> W _{1–<i>x</i>} Te ₂ Nanowhiskers: A Novel Electrocatalyst for Pt-Free Dye-Sensitized Solar Cells. ACS Applied Materials & Interfaces, 2020, 12, 34815-34824.	4.0	15
9	Synthesis of CoO-Decorated Graphene Hollow Nanoballs for High-Performance Flexible Supercapacitors. ACS Applied Materials & Interfaces, 2020, 12, 40426-40432.	4.0	32
10	The Study of HIV-1 Vpr-Membrane and Vpr-hVDAC-1 Interactions by Graphene Field-Effect Transistor Biosensors. ACS Applied Bio Materials, 2020, 3, 6351-6357.	2.3	2
11	Tin disulfide piezoelectric nanogenerators for biomechanical energy harvesting and intelligent human-robot interface applications. Nano Energy, 2020, 75, 104879.	8.2	40
12	Modulating Charge Separation with Hexagonal Boron Nitride Mediation in Vertical Van der Waals Heterostructures. ACS Applied Materials & Interfaces, 2020, 12, 26213-26221.	4.0	14
13	Spatial Confinement Approach Using Ni to Modulate Local Carbon Supply for the Growth of Uniform Transfer-Free Graphene Monolayers. Journal of Physical Chemistry C, 2020, 124, 23094-23105.	1.5	7
14	Tailoring of Effective Refractive Indices: A New Paradigm towards Ultralow Excitation Power of Upconversion Nanoparticles. , 2020, , .		0
15	Intracellular Delivery of Luciferase with Fluorescent Nanodiamonds for Dual-Modality Imaging of Human Stem Cells. Bioconjugate Chemistry, 2019, 30, 2228-2237.	1.8	19
16	High unsaturated room-temperature magnetoresistance in phase-engineered MoxW1â^'xTe2+δ ultrathin films. Journal of Materials Chemistry C, 2019, 7, 10996-11004.	2.7	9
17	Sn-Doping Enhanced Ultrahigh Mobility In _{1–<i>x</i>} Sn _{<i>x</i>} Se Phototransistor. ACS Applied Materials & Interfaces, 2019, 11, 24269-24278.	4.0	17
18	Nanoscale Core–Shell Hyperbolic Structures for Ultralow Threshold Laser Action: An Efficient Platform for the Enhancement of Optical Manipulation. ACS Applied Materials & Interfaces, 2019, 11, 1163-1173.	4.0	11

#	Article	IF	CITATIONS
19	Hybrid InSe Nanosheets and MoS ₂ Quantum Dots for Highâ€Performance Broadband Photodetectors and Photovoltaic Cells. Advanced Materials Interfaces, 2019, 6, 1801336.	1.9	23
20	Phaseâ€Engineered Weyl Semiâ€Metallic Mo _x W _{1â€x} Te ₂ Nanosheets as a Highly Efficient Electrocatalyst for Dyeâ€Sensitized Solar Cells. Solar Rrl, 2019, 3, 1800314.	3.1	14
21	Nanoscale Core-Shell Hyperbolic Structure: A New Paradigm to Boost the Light-Matter Interaction. , 2019, , .		Ο
22	One-step synthesis of graphene hollow nanoballs with various nitrogen-doped states for electrocatalysis in dye-sensitized solar cells. Materials Today Energy, 2018, 8, 15-21.	2.5	23
23	Lipid-Modified Graphene-Transistor Biosensor for Monitoring Amyloid-Î ² Aggregation. ACS Applied Materials & Interfaces, 2018, 10, 12311-12316.	4.0	21
24	Hepatocellular Carcinoma Diagnosis by DetectingÂα-Fucosidase with a Silicon Nanowire Field-Effect Transistor Biosensor. ECS Journal of Solid State Science and Technology, 2018, 7, Q3153-Q3158.	0.9	7
25	Transparent, Wearable, Broadband, and Highly Sensitive Upconversion Nanoparticles and Graphene-Based Hybrid Photodetectors. ACS Photonics, 2018, 5, 2336-2347.	3.2	59
26	A Highly-Efficient Single Segment White Random Laser. ACS Nano, 2018, 12, 11847-11859.	7.3	51
27	Highly Sensitive, Visible Blind, Wearable, and Omnidirectional Near-Infrared Photodetectors. ACS Nano, 2018, 12, 9596-9607.	7.3	62
28	Ultra-high performance flexible piezopotential gated In _{1â^`x} Sn _x Se phototransistor. Nanoscale, 2018, 10, 18642-18650.	2.8	13
29	The Extracellular Zn ²⁺ Concentration Surrounding Excited Neurons Is High Enough to Bind Amyloidâ€Î² Revealed by a Nanowire Transistor. Small, 2018, 14, e1704439.	5.2	7
30	Tuning Rashba Spin–Orbit Coupling in Gated Multilayer InSe. Nano Letters, 2018, 18, 4403-4408.	4.5	58
31	Epitaxial growth of vertically stacked p-MoS2/n-MoS2 heterostructures by chemical vapor deposition for light emitting devices. Nano Energy, 2017, 32, 454-462.	8.2	50
32	Detection of K+Efflux from Stimulated Cortical Neurons by an Aptamer-Modified Silicon Nanowire Field-Effect Transistor. ACS Sensors, 2017, 2, 69-79.	4.0	38
33	Targeted and efficient activation of channelrhodopsins expressed in living cells via specifically-bound upconversion nanoparticles. Nanoscale, 2017, 9, 9457-9466.	2.8	27
34	Detection of electrically neutral and nonpolar molecules in ionic solutions using silicon nanowires. Nanotechnology, 2017, 28, 165501.	1.3	2
35	Fluorescent nanodiamonds enable quantitative tracking of human mesenchymal stem cells in miniature pigs. Scientific Reports, 2017, 7, 45607.	1.6	68
36	One-Step Synthesis of Antioxidative Graphene-Wrapped Copper Nanoparticles on Flexible Substrates for Electronic and Electrocatalytic Applications. ACS Applied Materials & Interfaces, 2017, 9, 25067-25072.	4.0	21

#	Article	IF	CITATIONS
37	Acidity-activity correlation over bimetallic iron-based ZSM-5 catalysts during selective catalytic reduction of NO by NH3. Journal of Molecular Catalysis A, 2016, 423, 423-432.	4.8	31
38	Differential Releases of Dopamine and Neuropeptide Y from Histamineâ€Stimulated PC12 Cells Detected by an Aptamerâ€Modified Nanowire Transistor. Small, 2016, 12, 5524-5529.	5.2	20
39	Screening limited switching performance of multilayer 2D semiconductor FETs: the case for SnS. Nanoscale, 2016, 8, 19050-19057.	2.8	59
40	Ultraâ€Thin Layered Ternary Single Crystals [Sn(S <i>_x</i> Se _{1â^'} <i>_x</i>) ₂] with Bandgap Engineering for High Performance Phototransistors on Versatile Substrates. Advanced Functional Materials, 2016, 26, 3630-3638.	7.8	77
41	High photosensitivity and broad spectral response of multi-layered germanium sulfide transistors. Nanoscale, 2016, 8, 2284-2292.	2.8	129
42	Isolation and Identification of Post-Transcriptional Gene Silencing-Related Micro-RNAs by Functionalized Silicon Nanowire Field-effect Transistor. Scientific Reports, 2015, 5, 17375.	1.6	7
43	Tracking and Finding Slowâ€Proliferating/Quiescent Cancer Stem Cells with Fluorescent Nanodiamonds. Small, 2015, 11, 4394-4402.	5.2	36
44	Intrinsic Electron Mobility Exceeding 10 ³ cm ² /(V s) in Multilayer InSe FETs. Nano Letters, 2015, 15, 3815-3819.	4.5	354
45	Three-Dimensional Heterostructures of MoS ₂ Nanosheets on Conducting MoO ₂ as an Efficient Electrocatalyst To Enhance Hydrogen Evolution Reaction. ACS Applied Materials & Interfaces, 2015, 7, 23328-23335.	4.0	150
46	Growth of Large-Area Graphene Single Crystals in Confined Reaction Space with Diffusion-Driven Chemical Vapor Deposition. Chemistry of Materials, 2015, 27, 6249-6258.	3.2	72
47	Device Architecture and Biosensing Applications for Attractive One- and Two-Dimensional Nanostructures. , 2015, , 41-70.		1
48	Photoelectrochemical activity on Ga-polar and N-polar GaN surfaces for energy conversion. Optics Express, 2014, 22, A21.	1.7	26
49	(Invited) Nanowire Field-Effect Transistor-Based Biosensors as a Tool for Life Science. ECS Transactions, 2014, 64, 23-32.	0.3	Ο
50	Advances in nanowire transistors for biological analysis and cellular investigation. Analyst, The, 2014, 139, 1589.	1.7	52
51	High Performance and Bendable Few-Layered InSe Photodetectors with Broad Spectral Response. Nano Letters, 2014, 14, 2800-2806.	4.5	690
52	Binder-free rice husk-based silicon–graphene composite as energy efficient Li-ion battery anodes. Journal of Materials Chemistry A, 2014, 2, 13437-13441.	5.2	109
53	Wide-field imaging and flow cytometric analysis of cancer cells in blood by fluorescent nanodiamond labeling and time gating. Scientific Reports, 2014, 4, 5574.	1.6	80
54	Chemical Vapor Deposition Synthesis and Raman Spectroscopic Characterization of Large-Area Graphene Sheets. Journal of Physical Chemistry A, 2013, 117, 9454-9461.	1.1	57

#	Article	IF	CITATIONS
55	Biologically inspired graphene-chlorophyll phototransistors with high gain. Carbon, 2013, 63, 23-29.	5.4	100
56	An Ultrasensitive Nanowire-Transistor Biosensor for Detecting Dopamine Release from Living PC12 Cells under Hypoxic Stimulation. Journal of the American Chemical Society, 2013, 135, 16034-16037.	6.6	206
57	Improved silicon nanowire field-effect transistors for fast protein–protein interaction screening. Lab on A Chip, 2013, 13, 676-684.	3.1	25
58	A stable silicon/graphene composite using solvent exchange method as anode material for lithium ion batteries. Carbon, 2013, 63, 397-403.	5.4	50
59	Biomolecular recognition with a sensitivity-enhanced nanowire transistor biosensor. Biosensors and Bioelectronics, 2013, 45, 252-259.	5.3	86
60	Improving Nanowire Sensing Capability by Electrical Field Alignment of Surface Probing Molecules. Nano Letters, 2013, 13, 2564-2569.	4.5	49
61	Patterned growth of nanocrystalline silicon thin films through magnesiothermic reduction of soda lime glass. Green Chemistry, 2012, 14, 896.	4.6	19
62	Nanowire Transistorâ€Based Ultrasensitive Virus Detection with Reversible Surface Functionalization. Chemistry - an Asian Journal, 2012, 7, 2073-2079.	1.7	35
63	Monitoring extracellular K+ flux with a valinomycin-coated silicon nanowire field-effect transistor. Biosensors and Bioelectronics, 2012, 31, 137-143.	5.3	35
64	Changes in Plasma Membrane Surface Potential of PC12 Cells as Measured by Kelvin Probe Force Microscopy. PLoS ONE, 2012, 7, e33849.	1.1	24
65	High-Quality Graphene <i>pâ^'n</i> Junctions <i>via</i> Resist-free Fabrication and Solution-Based Noncovalent Functionalization. ACS Nano, 2011, 5, 2051-2059.	7.3	116
66	Photoinduced Electron Transfer in Dye‧ensitized SnO ₂ Nanowire Fieldâ€Effect Transistors. Advanced Functional Materials, 2011, 21, 474-479.	7.8	23
67	Silicon nanowire field-effect transistor-based biosensors for biomedical diagnosis and cellular recording investigation. Nano Today, 2011, 6, 131-154.	6.2	568
68	Structural, optical and luminescence studies of ZnSe nanowires. International Journal of Materials Research, 2011, 102, 1503-1506.	0.1	0
69	Surface potential variations on a silicon nanowire transistor in biomolecular modification and detection. Nanotechnology, 2011, 22, 135503.	1.3	31
70	Nanowire Field-effect Transistors and Their Applications to Cardiology. , 2011, , 45-57.		0
71	Label-free detection of protein-protein interactions using a calmodulin-modified nanowire transistor. Proceedings of the National Academy of Sciences of the United States of America, 2010, 107, 1047-1052.	3.3	115
72	Enhancement of the energy photoconversion efficiency through crystallographic etching of a c-plane GaN thin film. Journal of Materials Chemistry, 2010, 20, 8118.	6.7	23

#	Article	IF	CITATIONS
73	Dynasore inhibits rapid endocytosis in bovine chromaffin cells. American Journal of Physiology - Cell Physiology, 2009, 297, C397-C406.	2.1	21
74	Raman scattering of <scp>L</scp> â€ŧryptophan enhanced by surface plasmon of silver nanoparticles: vibrational assignment and structural determination. Journal of Raman Spectroscopy, 2009, 40, 150-156.	1.2	79
75	A reversible surface functionalized nanowire transistor to study protein–protein interactions. Nano Today, 2009, 4, 235-243.	6.2	82
76	Electron hopping conduction in highly disordered carbon coils. Carbon, 2009, 47, 1761-1769.	5.4	40
77	Observation of vibronically excited thioformaldehyde at 62,000–72,000cmâ^'1 by 1+1′+1′ resonance enhanced multiphoton ionization spectroscopy. Spectrochimica Acta - Part A: Molecular and Biomolecular Spectroscopy, 2008, 69, 27-32.	2.0	7
78	Exocytosis of a Single Bovine Adrenal Chromaffin Cell: The Electrical and Morphological Studies. Journal of Physical Chemistry B, 2008, 112, 9165-9173.	1.2	34
79	Ultrafast Spectroscopy Studies on Thickness Dependence of Acoustic Phonon Modes in Silver Nanoprisms. Journal of the Chinese Chemical Society, 2008, 55, 23-28.	0.8	2
80	Inâ€Situ Detection of Chromograninâ€A Released from Living Neurons with a Single-Walled Carbon-Nanotube Field-Effect Transistor. Small, 2007, 3, 1350-1355.	5.2	76
81	Lysophospholipids regulate excitability and exocytosis in cultured bovine chromaffin cells. Journal of Neurochemistry, 2007, 102, 944-956.	2.1	14
82	Solvothermal Preparation and Spectroscopic Characterization of Copper Indium Diselenide Nanorods. Journal of Physical Chemistry B, 2006, 110, 17370-17374.	1.2	86
83	Photoluminescence and Raman Scattering from Catalytically Grown ZnxCd1-xSe Alloy Nanowires. Journal of Physical Chemistry B, 2006, 110, 11691-11696.	1.2	98
84	Laser Assisted Catalytic Growth of ZnS/CdSe Core-Shell and Wire-Coil Nanowire Heterostructures. Journal of the Chinese Chemical Society, 2005, 52, 725-732.	0.8	7
85	Photosynthesis of Gold Nanoparticles in Presence of Proteins. Journal of Nanoscience and Nanotechnology, 2005, 5, 2128-2132.	0.9	12
86	Two-photon vibronic spectroscopy of allene at 7.0–10.5 eV: experiment and theory. Molecular Physics, 2005, 103, 229-248.	0.8	1
87	Surface-Enhanced Raman Scattering and Polarized Photoluminescence from Catalytically Grown CdSe Nanobelts and Sheets. Journal of the American Chemical Society, 2005, 127, 11262-11268.	6.6	142
88	Synthesis and properties of carbon nanospheres grown by CVD using Kaolin supported transition metal catalysts. Carbon, 2004, 42, 813-822.	5.4	144
89	High-lying Rydberg states of vinyl bromide studied by two-photon resonant ionization spectroscopy. Chemical Physics Letters, 2004, 394, 287-292.	1.2	4
90	Effect of TiO2 Nanoparticles on the Improved Surface-Enhanced Raman Scattering of Polypyrrole Deposited on Roughened Gold Substrates. Journal of Physical Chemistry B, 2004, 108, 14897-14900.	1.2	33

#	Article	IF	CITATIONS
91	Catalytic Growth of Silicon Nanowires Assisted by Laser Ablation. Journal of Physical Chemistry B, 2004, 108, 846-852.	1.2	91
92	Applications and Advances of Resonance-Enhanced Multiphoton Ionization Spectroscopy. ChemInform, 2003, 34, no.	0.1	0
93	One- and two-photon excitation vibronic spectra of 2-methylallyl radical at 4.6–5.6 eV. Journal of Chemical Physics, 2003, 119, 241-250.	1.2	13
94	Optical Properties of Host(SBAâ€15)â€guest(AgI) Composite Materials. Journal of the Chinese Chemical Society, 2003, 50, 59-64.	0.8	1
95	Two-photon resonant ionization spectroscopy of the allyl-h5 and allyl-d5 radicals:  Rydberg states and ionization energies. Journal of Chemical Physics, 2002, 116, 4162-4169.	1.2	19
96	Molecular Rydberg States and Ionization Energy Studied by Twoâ€Photon Resonant Ionization Spectroscopy. Journal of the Chinese Chemical Society, 2002, 49, 703-722.	0.8	1
97	Time-resolved photoluminescence study of silica nanoparticles as compared to bulk type-III fused silica. Physical Review B, 2002, 66, .	1.1	94
98	Ab initio calculations of low-lying electronic states of vinyl chloride. Journal of Chemical Physics, 2002, 116, 7518-7525.	1.2	24
99	Red and near-infrared photoluminescence from silica-based nanoscale materials: Experimental investigation and quantum-chemical modeling. Journal of Chemical Physics, 2002, 116, 281.	1.2	44
100	Photoluminescence from mesoporous silica akin to that from nanoscale silicon: the nature of light-emitters. Chemical Physics Letters, 2002, 358, 180-186.	1.2	41
101	Size effect in self-trapped exciton photoluminescence fromSiO2-based nanoscale materials. Physical Review B, 2001, 64, .	1.1	109
102	A New Sub-Doppler Fluorescence Imaging Method in Studying Laser Ablation of B Atoms at 248 nm. Journal of Physical Chemistry B, 2001, 105, 5079-5082.	1.2	0
103	Investigations of Ultrafast Exciton Dynamics in Allophycocyanin Trimerâ€. Journal of Physical Chemistry A, 2001, 105, 8878-8891.	1.1	20
104	Study of Photodissociation Dynamics Using Subâ€Đoppler Fluorescence Imaging Method: Photodissociation of ICN at 308 nm. Journal of the Chinese Chemical Society, 2001, 48, 619-624.	0.8	1
105	Vibronic spectra of the allyl radical at 6–8 eV with resonance-enhanced multiphoton ionization technique. Science in China Series B: Chemistry, 2001, 44, 360-365.	0.8	1
106	Studies on the multiphoton ionization spectrum of the jet-cooled acetyl radical at 6.2–7.6 eV. Chemical Physics, 2001, 274, 275-281.	0.9	9
107	Photoluminescence properties of silica-based mesoporous materials similar to those of nanoscale silicon. European Physical Journal D, 2001, 16, 279-283.	0.6	15
108	Two-photon vibronic spectra of vinyl chloride at 7.3–10 eV. Journal of Chemical Physics, 2001, 115, 5925-5931.	1.2	14

#	Article	IF	CITATIONS
109	Computational formulas for symmetry-forbidden vibronic spectra and their application to n–i̇́€* transition in neat acetone. Journal of Chemical Physics, 2001, 115, 4080-4094.	1.2	25
110	High-lying Rydberg states and ionization energy of vinyl chloride studied by two-photon resonant ionization spectroscopy. Chemical Physics Letters, 2000, 325, 369-374.	1.2	17
111	Determination of velocity distribution, angular distribution, and vector correlation of photofragments using sub-Doppler fluorescence-imaging method. Journal of Chemical Physics, 2000, 113, 5716-5724.	1.2	2
112	Rydberg states of the allyl radical observed by two-photon resonant ionization spectroscopy. Journal of Chemical Physics, 2000, 113, 7286-7291.	1.2	23
113	Photoluminescence from mesoporous silica: Similarity of properties to porous silicon. Applied Physics Letters, 2000, 77, 3968-3970.	1.5	56
114	Rydberg states of propyne at 6.8–10.5 eV studied by two-photon resonant ionization spectroscopy and theoretical calculation. Journal of Chemical Physics, 2000, 112, 7384-7393.	1.2	30
115	Power Laser Ligh-Induced Photoluminescence from Detonation-Synthesized 5nm-Sized Diamonds. Defect and Diffusion Forum, 2000, 186-187, 37-44.	0.4	0
116	Photoluminescence Spectroscopy of Silica-Based Mesoporous Materials. Journal of Physical Chemistry B, 2000, 104, 8652-8663.	1.2	61
117	Two-photon-excited luminescence and defect formation in SiO2 nanoparticles induced by 6.4-eV ArF laser light. Physical Review B, 2000, 62, 4733-4743.	1.1	140
118	Photodissociation of propyne and allene at 193 nm with vacuum ultraviolet detection of the products. Journal of Chemical Physics, 1999, 110, 3320-3325.	1.2	39
119	Ab initio study of the n-ï€* electronic transition in acetone: Symmetry-forbidden vibronic spectra. Journal of Chemical Physics, 1999, 111, 205-215.	1.2	58
120	The photoluminescence from hydrogen-related species in composites of SiO2 nanoparticles. Applied Physics Letters, 1999, 75, 778-780.	1.5	152
121	The Fragmentation of Melamine:Â A Study via Electron-Impact Ionization, Laser-Desorption Ionization, Collision-Induced Dissociation, and Density Functional Calculations of Potential Energy Surface. Journal of Physical Chemistry B, 1999, 103, 582-596.	1.2	25
122	Ionization and Emission Spectra of the Photofragments of Allene Excited at 193 nm. Journal of Physical Chemistry A, 1999, 103, 6063-6073.	1.1	4
123	Power dependence of transient degenerate four-wave mixing in molecular systems. Physical Review A, 1997, 55, 3086-3091.	1.0	1
124	Theoretical Study of the Structure, Energetics, and the nâ^'Ï€* Electronic Transition of the Acetone +nH2O (n= 1â^'3) Complexes. Journal of Physical Chemistry A, 1997, 101, 9925-9934.	1.1	36
125	IR spectroscopy and theoretical vibrational calculation of the melamine molecule. Journal of the Chemical Society, Faraday Transactions, 1997, 93, 3445-3451.	1.7	81
126	Ab initio molecular orbital study of excited electronic states of the vinyl radical. Chemical Physics Letters, 1997, 275, 19-27.	1.2	47

#	Article	IF	CITATIONS
127	On the theoretical investigation of vibronic spectra of ethylene by ab initio calculations of the Franck–Condon factors. Journal of Chemical Physics, 1996, 105, 9007-9020.	1.2	68
128	Ï€-Ï€â^— vibronic spectrum of ethylene from ab initio calculations of the Franck-Condon factors. Chemical Physics Letters, 1996, 258, 53-62.	1.2	57
129	Theoretical study of isomeric structures and low-lying electronic states of the vinyl radical C2H3. Chemical Physics, 1996, 206, 43-56.	0.9	42
130	Transient degenerate four-wave mixing in molecular systems. Optical and Quantum Electronics, 1996, 28, 1477-1493.	1.5	3
131	Stimulated emission pumping spectroscopy of HCP near the isomerization barrier: EVIBâ‰⊉5 315 cmâ^1. Journal of Chemical Physics, 1996, 105, 7383-7401.	1.2	42
132	Laser-Induced Fluorescence Excitation Spectroscopy of Highly Vibrationally Excited Ã2A1 NH2 Radical. Journal of Molecular Spectroscopy, 1995, 169, 427-439.	0.4	3
133	Theoretical vibrational and rotational energies and intensities of the HNSi and DNSi molecules. Journal of Chemical Physics, 1993, 98, 1352-1357.	1.2	17
134	Comparison of theoretical vibrational and rotational energies of the HCP molecule with experimental values. Journal of Chemical Physics, 1993, 99, 8870-8876.	1.2	11
135	Ultraviolet laser-induced fluorescence of the C2H radical. Chemical Physics Letters, 1992, 190, 507-513.	1.2	15
136	Observation of highly vibrationally excited X̃ 1Σ+ HCP by stimulated emission pumping spectroscopy. Journal of Chemical Physics, 1990, 93, 2149-2151.	1.2	37
137	On the anomalous A1–A2 splittings in the ν2-ν4 manifold of PH3. Journal of Molecular Spectroscopy, 1989, 133, 148-156.	0.4	15
138	Stark and Zeeman effects in ethylene observed by subâ€Đoppler infrared spectroscopy. Journal of Chemical Physics, 1988, 88, 5282-5290.	1.2	18
139	Sub-Doppler spectroscopy using a multiple-reflection mirror system. Journal of the Optical Society of America B: Optical Physics, 1986, 3, 935.	0.9	11
140	Observation of ground state rotational transitions in silicon tetrafluoride. Journal of Molecular Spectroscopy, 1986, 120, 233-235.	0.4	17